JOURNAL OF APPLIED ELECTROCHEMISTRY **26** (1996) 343–352

Performance and thermodynamic properties of Na–Sn and Na–Pb molten alloy electrodes for alkali metal thermoelectric converter (AMTEC)

Q. FANG

Department of Materials Science and Engineering, University of Science and Technology of China Hefei Anhui 230026, China

H. WENDT

Institut für Chemische Technologie, Technische Hochschule Darmstadt, Petersen Str. 20, 64287 Darmstadt, Germany

Received 26 June 1995; revised 14 August 1995

An alkali metal thermoelectric converter (AMTEC) testing cell was set up, and run with molten sodium–tin (Na–Sn) and sodium–lead (Na–Pb) alloy cathodes. The Na activity, the partial molar enthalpy and partial molar entropy of sodium in molten Na–Sn and Na–Pb alloys have been determined, using a Na concentration cell: Na(l)|beta″-alumina|Na–Me(l), where Me = Sn or Pb. The thermodynamic results of these investigations agree with those of other authors. The electric performance of these Na–Me alloy electrodes of different Na concentration and temperatures is described, measuring current–voltage characteristics and a.c. impedance in the AMTEC test cell. The power density of the AMTEC cell with molten alloy cathodes decreases with increasing Na concentration, with the Na concentrations in molten alloys varying from 0.5 to 15 mol %. Maximum power densities of 0.21 to 0.15 W cm^{-2} at 700 °C for Na–Sn molten electrodes, and 0.30 to 0.15 W cm^{-2} for Na–Pb molten electrodes have been obtained. The a.c. impedance data demonstrated that the molten alloy electrodes have a smaller cell resistance, 0.3–0.35 Ω cm^{-2} at 700 °C after 10–20 h. Comparison with the sputtered thin, porous film electrodes, showed that the contact resistance between electrode and surface of beta″-alumina plays an important role on enhancing cell power density. At 700 °C the power density of an AMTEC cell with the molten Na–Pb alloy electrode can be raised to values of about 0.2 W cm^{-2}at current densities of 0.8 A cm^{-2}, but at cell voltages not exceeding 0.2 V. A model for the theoretical efficiency of the AMTEC cell with molten Na metal electrodes is also presented.

1. Introduction

The alkali metal thermoelectric converter (AMTEC) is a system in which beta″-alumina acts as a solid sodium ion conducting electrolyte. Sodium is used as the working medium, for direct conversion of heat into electricity [1–8]. Its main advantages are believed to be high efficiency, high power density, modular design, low maintenance and low manufacturing cost. An AMTEC cell with an efficiency of 19% [9, 10], lifetimes to 10 000 h [3, 4], and cell power density up to 1 W cm^{-2} [11] has been reported. With a 36 cell module, an electric power of 550 W was achieved [12].

The AMTEC essentially consists of two compartments: a high-pressure compartment, where sodium is heated from 500 to 1000° C, and a low-pressure compartment, where sodium vapour is condensed at a temperature of about 300 °C, corresponding to a sodium saturated vapour pressure of about 10^{-5} bar. Electricity is generated in the AMTEC by sodium ion transport through beta″-alumina from the high-pressure to the low-pressure compartment, while electrons flow through the load. The driving force for this process is the pressure difference between the two compartments. Ionization of sodium metal and recombination of the sodium ions and electrons, according to Equation 1, take place at the electrolyte/electrode interfaces on either side of the solid state electrolyte:

$$\mathrm{Na} \Longleftrightarrow \mathrm{Na}^{+} + \mathrm{e}^{-} \qquad (1)$$

The anode is normally liquid sodium metal, and the cathode usually is a layer of porous, refractory metal or compound such as Mo, W or TiN and TiB_2. Porous molybdenum cathodes, show high initial power densities but degrade to a 'mature' state with strong reduction in power and efficiency after 10 to 1000 h [9, 10, 13]. The major reason of the transient degradation of molybdenum electrode is loss of sodium molybdates, which form only molybdenum oxides within the electrode, improve the performance initially and disappear eventually by evaporation

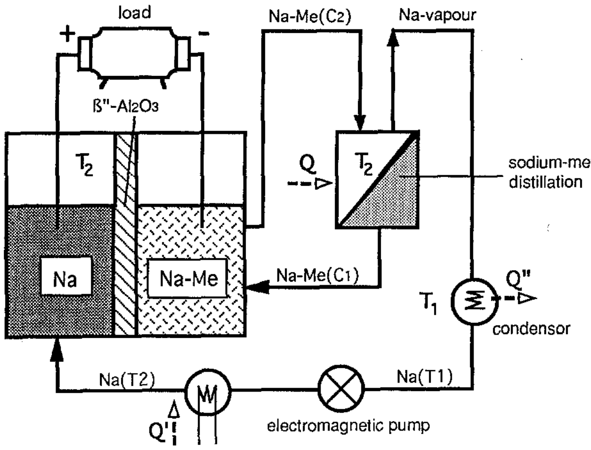

Fig. 1. Schematic diagram of an AMTEC system with Na–Me electrode.

(e.g., m.p. of Na_2MoO_4 is 687 °C). To improve the stability of AMTEC cells, further work has been carried out with TiN and TiB_2 thin films as electrodes [8, 13, 14]. The results from sputtered Mo, TiN and TiB_2 thin-film electrodes indicated that the power density of an AMTEC cell depends not only on thickness, porosity and electric conductivity of the metal film, but also on the electrode/electrolyte contact, and the good connection between electrode and current collector [15, 16]. It is therefore desirable to eliminate such contact resistances by using sodium alloys with different sodium metal activities on both sides of the solid electrolyte.

This paper describes an investigation of the thermodynamic properties of molten Na–Me alloys, assessing the performance of AMTEC cells with Na–Me molten alloy electrodes, determining the influence of the contact and interface-resistance between the molten metal electrode and electrolyte as an alternative AMTEC technology, and enhancing the power density of this electricity generating device.

Figure 1 shows the schematic of an AMTEC-system with molten Na–Me alloy electrode. T_2 is the higher temperature and T_1 is the lower temperature in the AMTEC system. Sodium and sodium alloy, which are separated by a beta″-alumina solid electrolyte, are kept at the higher temperature T_2. The driving force for this type of AMTEC is the difference in sodium activity between sodium and the sodium alloy reservoir. Electricity is generated by sodium ion transport through beta″-alumina from sodium side, the high Na activity side, to the Na alloy side, while electrons flow through the load.

To maintain cycling of the working medium in the system and to separate pure sodium from sodium alloy, a sodium alloy distillation system and a condenser are necessary. The condensed sodium is pumped into a Na reservoir by an electromagnetic pump.

To calculate the thermal equilibrium conveniently, the evaporation of sodium from the liquid alloy at T_2 is known as Q, Q' is the energy of heating sodium from T_1 to T_2 and Q'' is the released heat of Na vapour to the condenser at T_1.

Table 1. Some physical properties of tin and lead

	Tin	*Lead*	*References*
m.p./° C	231.9	327.5	[17]
Resistivity/$\mu\Omega$ cm	11.0	20.65	[18]
Vapour pressure	1 torr/1600 °C	1 torr/973 °C	[19]
Na solubility	2.4 at % (at 493 °C)	4.1–18 at % (at 580 °C)	[20]

Since molten sodium metal and sodium alloys contact both sides of the beta″-alumina solid electrolyte and the driving force for this process is the difference in Na-activity between the faces of the solid electrolyte, one of the advantages is that the vacuum system, which is usually used in AMTEC cells with porous thin film cathodes, is not necessary. Second, the charge transfer at the interface of Na–Me molten electrode/alumina is much simpler, compared to the electrode process in porous, thin film electrodes, which includes interfacial transfer of Na^+ ions, and electrochemical reactions and diffusion of Na gas in the holes of the electrode. However, separating sodium and the alloying metals is a particular problem in this type of process.

Tin and lead have been selected as alloying metals, because these metals have low melting points, good electric conductivities, relative low vapour pressures, suitable Na solubility and low Na activity and vapour pressure in Na–Me alloys whose sodium concentration do not exceed 30%. Table 1 shows some physical properties of tin and lead.

Mathewson [20] studied the phase diagram of Na–Pb in Na concentration between 1 to 94 at %. There are four eutectic points with four melting point maxima, due to compound formation. The phase diagram of Na–Sn displays a eutectic point at about 5 at % Na with a melting point depression of 12 °C. It also shows melting point maxima at higher Na concentration, due to the compounds $NaSn_6$, NaSn, Na_2Sn and Na_4Sn [21].

In this paper, the following subjects had been investigated experimentally:

(i) Determination of thermodynamic data for molten Na–Sn and Na–Pb alloys by e.m.f. measurement in a sodium concentration cell at temperatures from 400 to 700 °C, and with Na concentrations of 0.5 to 25 at %.
(ii) Measurement of the current–voltage characteristics and power density of an AMTEC cell with Na alloys of Pb and Sn with various Na concentrations.
(iii) Investigating the electrode process and contact-resistance between beta″-alumina and liquid alloy electrode at various temperatures and Na concentrations.
(iv) Comparing AMTEC cells with alloy electrodes with AMTEC cells, equipped with the sputtered Mo, TiN and TiB_2 thin film electrodes by impedance spectroscopy.

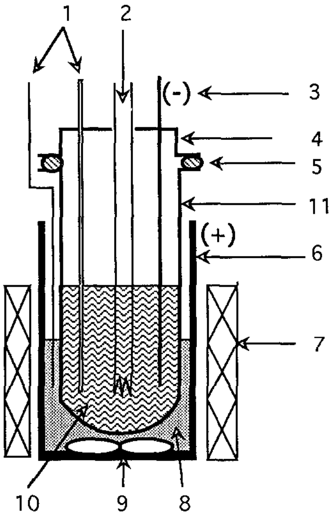

Fig. 2. Schematic diagram of Na–Me electrode test cell. Key: (1) thermocouple, (2) internal heater and current collector, (3) terminal for voltage measurement, (4) steel cover, (5) rubber O-ring seal, (6) steel tube (+ve terminal) and current collector, (7) external oven, (8) Sn or Pb, (9) electromagnetic mixer, (10) sodium and (11) beta″-alumina.

2. Experimental details

2.1 *Testing cell*

Figure 2 shows the schematic of an AMTEC-cell with a molten Na-alloy electrode, which was set up in a nitrogen filled glove box. The solid electrolyte consisted of a beta″-alumina tube 200 mm long, 25 mm in diameter, with a 1.3 mm wall thickness obtained from BAT (high energy battery), ABB AG. This tube was inserted in a steel tube of 80 mm long and 28 mm inner diameter. Liquid sodium (20–30 g) was placed into the alumina tube, which was equipped with an electric heater. A maximum internal temperature of 750 °C was achieved. The upper end of the β''-Al_2O_3 tube, which had been fit an alumina ceramic ring, was sealed by a rubber O-ring seal to a steel cover.

An amount of 2.5 moles of the molten pure alloying liquid metal (tin or lead) was placed in the steel tube. On the bottom of the steel tube, an electromagnetic stirrer was used to homogenize the molten alloys during the experiment.

A current collector (stainless steel tube 10 mm dia.) was immersed into the liquid sodium (anode) at the centre of the beta″-aluminium oxide tube, while the molten alloys or Na-metal alloys were connected to the steel vessel which served as the current lead.

The e.m.f. between Na and the alloy electrode was measured with a digital multifunction meter (BBC M2110). The current supplying the pure Na from the sodium electrode to alloy electrode by coulometric titration, came from a power supply (IEEE-488 interface, Elba-modul GMBH).

Current–voltage curves were measured under steady state condition. The cell impedances were determined with an impedance-measuring instrument (Zahner Elektrik IM 5d).

Table 2. Contact resistances of the cell with molten electrode by 700 °C

Time/min	*5*	*30*	*60*	*120*	*180*	*240*	*300*
R_c of Sn/$\Omega\,cm^2$	1.10	0.80	0.65	0.58	0.50	0.48	0.48
R_c of Pb/$\Omega\,cm^2$	1.20	1.00	0.85	0.76	0.68	0.65	0.64

The β''-Al_2O_3 tube was immersed into the molten Sn or Pb to a depth of 0.25–2 cm. The β''-Al_2O_3 tube has a diameter of 2.5 cm and a semispherical bottom, accordingly, an electrode areas from 0.5 to 15 cm^2 were obtained, depending on the amount of alloy.

The temperatures of sodium and sodium alloys were measured with a nickel–chromium/nickel thermocouple. The sodium alloys were prepared by two different methods: (a) *ex situ* using pure sodium and tin or lead in a nitrogen atmosphere and (b) *in situ* by coulometric transfer of sodium through the cell into pure molten Sn or Pb-metal.

2.2. *Wetting of the electrolyte*

Before each investigation of the cell, the β''-Al_2O_3 tube was carefully cleaned in an ultrasonic bath filled with pure ethanol and subsequently heated to 400° C in a vacuum furnace. It is worth noting that wetting of the solid state electrolyte by molten metal (Sn or Pb) or molten alloys is of highest importance. The relatively high impedance of the cell which is measured immediately after setup of the cell shows that in the beginning the beta″-alumina is only poorly wetted. A better wetting of the electrolyte tube and lower contact-resistance between electrolyte and molten electrode could be obtained by longer heating or by flowing current for a longer time of cell operation. Table 2 shows the effects at 700 °C, within 60 mins, where the cell resistance decreases from 1.1 or 1.2 $\Omega\,cm^2$ to 0.65 or 0.85 $\Omega\,cm^2$, respectively, and thereafter still drops to 0.5 or 0.6 $\Omega\,cm^2$.

2.3. *Chemical stability of the electrolyte*

After the electrochemical tests, the microstructures and chemical composition of the used beta″-alumina electrolyte were investigated by scanning electron microscopy (SEM) and energy dispersion spectroscopy (EDS). The e.m.f. measurements, current–voltage testing and charge or discharge in this AMTEC cell, which usually lasted for more than 30 h, were found by SEM and EDS that neither Sn nor Pb was introduced into the β''-alumina electrolyte by ion exchange.

3. Thermodynamic investigation of sodium-metal alloys

3.1 *E.m.f. measurement*

The e.m.f. of the concentration cell, Na(l)|β''-alumina electrolyte|Na–Me-alloy(l), was measured across a

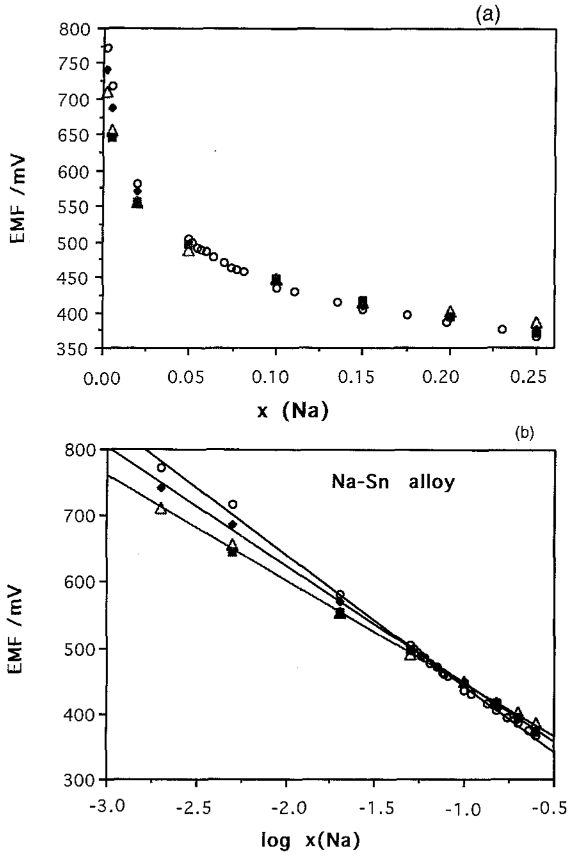

Fig. 3. Dependence of e.m.f. for Na–Sn molten alloy on the sodium concentration. (a) Direct relation; (b) semilogarithmic relation. Key: (○) E-700, (◆) E-600, (△) E-500 and (■) ITOH-455 °C [22].

temperature range from 400 to 700 °C and sodium concentration in the alloy ranging from a mole fraction of 0.005 to 0.25. Since the transport number of sodium cations in β''-alumina electrolyte, $t^+(\mathrm{Na}) = 1$, the e.m.f. of the concentration cell reads:

$$E = \frac{RT}{F} \ln \left(\frac{a_0}{a_{\mathrm{Na}}} \right) \tag{2}$$

where a_{Na} is the Na activity in the sodium alloy and a_0 is the Na activity in pure liquid sodium is 1. Accounting for the activity coefficient of sodium in the alloy, f_i, the Na-activity a_i is obtained by multiplying the mole fraction x_i with f_i:

$$a_i = f_i x_i \tag{3}$$

Figures 3(a) and (b) show the dependence of the e.m.f. for Na–Sn alloys at 500, 600 and 700 °C on the Na concentration in a linear and a semilogarithmic plot, comparing them with the data measured by Itoh at 445 °C [22].

From Fig. 3(b), slopes $(\mathrm{d}E/\mathrm{d}\log a)$, of -198, -178 and $-156\,\mathrm{mV\ decade^{-1}}$ for the three temperatures are obtained. Theoretically, slopes of -193, -173 and $-154\,\mathrm{mV\,decade^{-1}}$ for the temperature of 700, 600 and 500 °C are expected, assuming ideal behaviour of the alloys or concentration-independent activity coefficients for sodium and tin alloy.

Figures 4(a) and (b) show the same correlation for Na–Pb alloys. Slopes of -194, -178 and $-163\,\mathrm{mV}$ are obtained for 700, 600 and 500 °C. Again the slopes indicate almost ideal mixtures or concentration-independent activity coefficient.

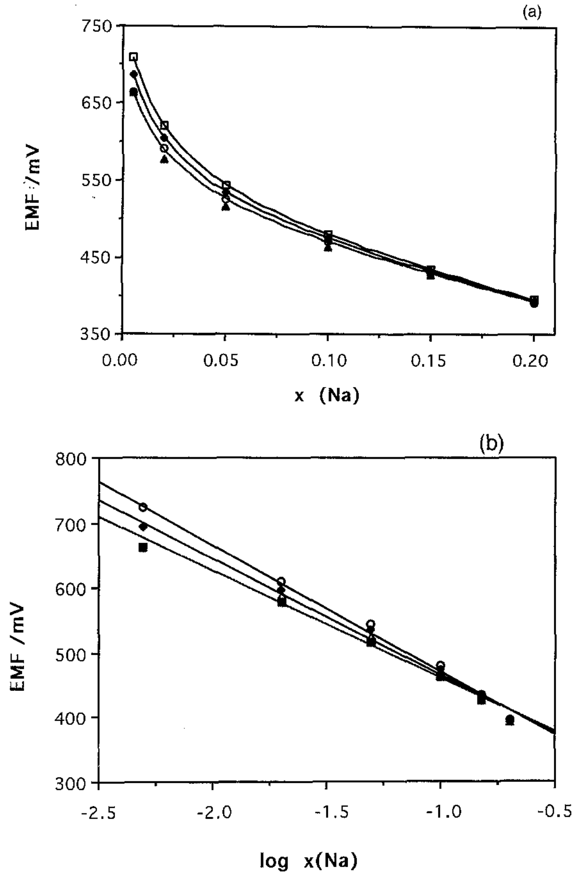

Fig. 4. Dependence of e.m.f. for Na–Pb molten alloy on the sodium concentration. (a) Direct relationship; (b) semilogarithmic relationship. Temperatures for (a): (□) 700, (◆) 600, (○) 500 and (▲) 410 °C [23]; temperatures for (b): (○) 700, (◆) 600, (△) 500 and (■) 410 °C [23].

3.2. *Thermodynamics of molten Na–Sn and Na–Pb alloys*

The temperature dependence of the equilibrium potentials (E) of the $\mathrm{Na}|\beta''\text{-}\mathrm{Al_2O_3}|\mathrm{Na{-}Me}$ cells with constant Na concentration, is linear for temperatures more than 400 °C, according to the relation

$$E = A + kT \tag{4}$$

where A and k are constants, with

$$\Delta G_{\mathrm{Na}} = -nFE \tag{5}$$

and

$$\Delta G_{\mathrm{Na}} = \Delta H_{\mathrm{Na}} - \Delta S_{\mathrm{Na}} T \tag{6}$$

The partial molar enthalpy, ΔH_{Na}, and entropy, ΔS_{Na}, of sodium in the liquid alloy may be obtained by evaluating the quantity A from the E/T plots:

$$\Delta H_{\mathrm{Na}} = -FA \tag{7}$$

and

$$\Delta S_{\mathrm{Na}} = kF \tag{8}$$

Figure 5 shows the temperature dependence of the e.m.f.s for different sodium concentrations in Na–Sn

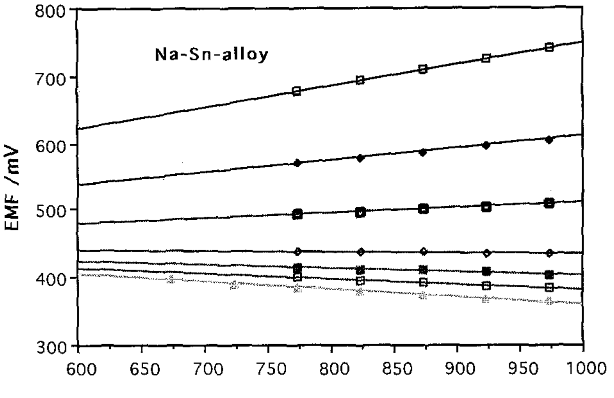

Fig. 5. Temperature dependence of e.m.f. for sodium concentration cell with Na–Sn electrode. Key: (□) $E(0.005)$, (◆) $E(0.02)$, (▣) $E(0.05)$, (◇) $E(0.10)$, (■) $E(0.15)$, (□) $E(0.20)$ and (▲) $E(0.25)$.

alloys with mole fractions $5\times10^{-3}\leq x\leq0.25$ and the temperature range from 400 to 700 °C. For low Na concentration (up to $x=0.05$), the E/T straight lines have a positive slope; in the higher Na concentration ($x>0.1$), the slope $\mathrm{d}E/\mathrm{d}T$, equalling ΔS is negative. Table 3 shows the calculated values of the section A and the slope k from the E/T plot of the $\mathrm{Na}/\beta''\text{-}\mathrm{Al_2O_3}|\mathrm{Na\text{-}Me}$ (Me = Sn, Pb) cell, for the temperature from 500 to 700 °C.

The experimental results of the molten Na–Pb alloys are depicted in Fig. 6. In this case only positive k values, corresponding to ΔS_{Na} for the molten Na–Pb alloys with sodium mole fractions $5\times10^{-3}\leq x\leq 0.20$ and the temperature range from 500 to 700 °C, are observed.

3.2.1. Dependence of ΔS_{Na} on Na concentration.

Figure 7 compares the partial molar entropies of sodium in Na–Sn and Na–Pb alloys with the partial molar entropy of ideal mixtures, $R\ln x$. In both alloys (tin and lead) the partial entropies vary with the function $\log x(\mathrm{Na})$, as they are more negative. In Na–Pb alloys, the deviation from ideality decreases with the sodium concentration, while in Na–Sn alloys, the deviation increases slightly with the sodium concentration.

In the formation of the molten Na–Sn alloys exist two opposite effects on the entropy ΔS_{Na}: one is a dissolution effect of sodium in alloys; and another is an orientation or short-range order effect, which results from the formation of Na–Sn compounds. In the case of the dissolution process, a definitely positive part is contributed to the ΔS_{Na}; while a negative part is given in the other case of the formation of Na–Sn compounds. Therefore, the negative E/T temperature coefficient for the higher Na concentration range (from 5 at %) implies that the effect of compound formation is predominant in higher Na concentration for Na–Sn alloys.

Table 3. A and k values from E/T curve for 500–700 °C

x_{Na}	*Sn*		*Pb*	
	A/mV	k/mV K^{-1}	A/mV	k/mV K^{-1}
0.005	431 ± 2	0.32 ± 0.01	482 ± 2	0.23 ± 0.01
0.02	429 ± 2	0.18 ± 0.01	483 ± 2	0.14 ± 0.01
0.05	431 ± 1	0.08 ± 0.005	452 ± 1	0.095 ± 0.005
0.10	445 ± 1	−0.01 ± 0.002	427 ± 1	0.055 ± 0.002
0.15	455 ± 1	−0.05 ± 0.005	410 ± 1	0.025 ± 0.002
0.20	462 ± 1	−0.08 ± 0.005	381 ± 1	0.015 ± 0.002
0.25	471 ± 1	−0.11 ± 0.01		

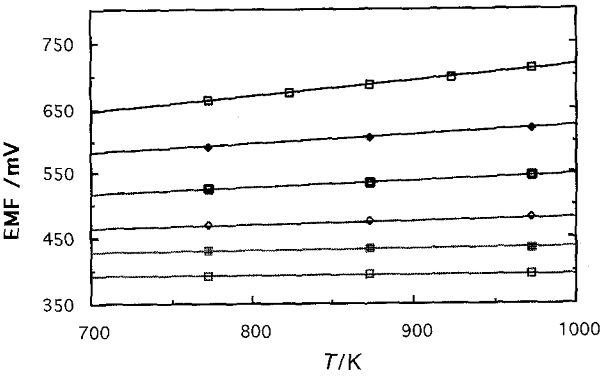

Fig. 6. Temperature dependence of e.m.f. for sodium concentration cell with Na–Pb electrode. Key: (□) $E(0.005)$, (◆) $E(0.02)$, (□) E (0.05), (◇) $E(0.10)$, (■) $E(0.15)$, (□) $E(0.20)$ (top and bottom).

3.2.2. Dependence of ΔH_{Na} on Na concentration.

Figure 8 shows the partial molar enthalpy ΔH_{Na}, which is the molar enthalpy of dissolution of sodium in Na–Sn and Na–Pb alloys. $\Delta H_{\mathrm{Na}}$for both Na–Sn and Na–Pb alloys are negative, and are of the same order of magnitude. The slopes of $\mathrm{d}\Delta H_{\mathrm{Na}}/\mathrm{d}x$ in Na–Pb and Na–Sn alloys are opposite. The partial molar heat of sodium diminishes strongly with increasing Na concentration in sodium lead alloys, whereas it increases slightly with the Na concentration in Na–Sn alloys.

3.2.3. Sodium activity coefficient in Na–Me alloys.

According to Equation (3), the activity coefficient of sodium in Na–Me alloys $f_i(x,T)$ is calculated from the e.m.f. values. Figure 9 shows the concentration dependence of the activity coefficient of sodium f_i in Na–Sn alloys versus the molar fraction x_{Na} at various temperatures between 500 and 700 °C. The activity coefficient of sodium in Na–Sn alloys at

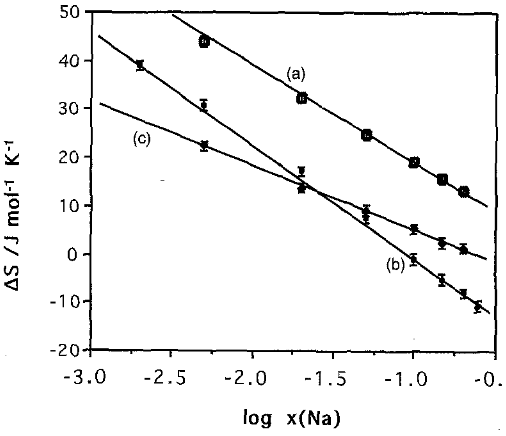

Fig. 7. Sodium concentration dependence of ΔS_{Na} in Na–Me alloys. Key: (a) ΔS(th), (b) ΔS(Na–Sn) and (c) ΔS(Na–Pb).

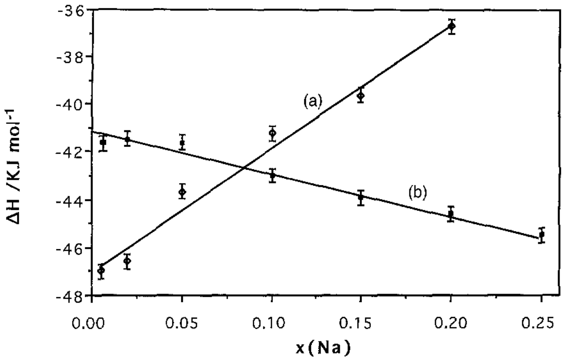

Fig. 8. Sodium concentration dependence of ΔH_{Na} in Na–Me alloys. Key: (a) ΔH(Na–Pb) and (b) ΔH(Na–Sn).

455 °C from Itoh [22] is also given. After a slight increase of f_i in the concentration range $0 < x < 0.05$, the activity coefficient of sodium in Na–Sn alloys remains almost constant up to $x = 0.25$.

The activity coefficient of sodium in Na–Pb alloys f_i against $X_{\mathrm{Na}}$is shown in Fig. 10. Quite differently the activity coefficient of sodium in molten Na–Pb alloys increases at higher sodium concentration.

3.3. *Discussion*

These experimental results can be explained by the Na–Sn and Na–Pb phase diagram [20]. The first eutectic point in the Sn-rich side is at about 5 at % Na, the melting point of the Na–Sn alloys drops by about 12 °C with increasing Na concentration. The Na–Sn compounds in molten Na–Sn alloys will be formed when sodium concentration is over 5 at %. The first eutectic point of Na–Pb alloys in the Pb-rich side is at about 22 at % and the melting point of the Na–Pb alloys drops about 20 degrees in temperature.

Figures 5 and 6 show that the e.m.f. against temperature for Na–Me electrodes displays straight lines. The slopes of E/T plotting for both alloys decrease with increasing Na concentration monotonously. However, the difference between both alloys is that the slope $k = \mathrm{d}E/\mathrm{d}T$ for Na–Pb alloy even at 20 at % Na keeps positive (see Table 3). Obviously, the effect of compound formation in Na–Pb molten alloys is weaker than that in Na–Sn alloys.

The thermodynamic findings help to design an AMTEC with molten alloy electrodes. Obviously Na–Pb alloys are better suited than Na–Sn alloys because at the same temperature and Na concentration, the sodium activity in Na–Pb alloys is lower than that in Na–Sn alloys.

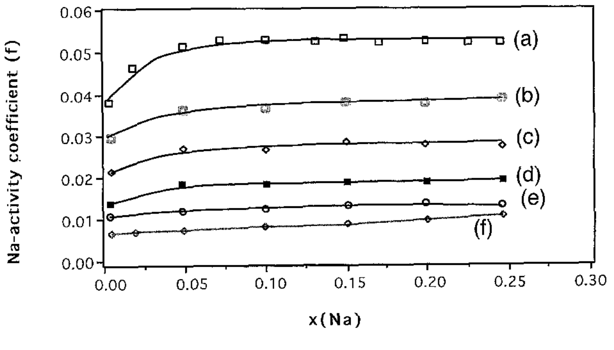

Fig. 9. Sodium activity coefficient, f_i, in Na–Sn alloys against x_{Na}. Temperatures: (a) 700, (b) 650, (c) 600, (d) 550, (e) 500 and (f) 455 °C.

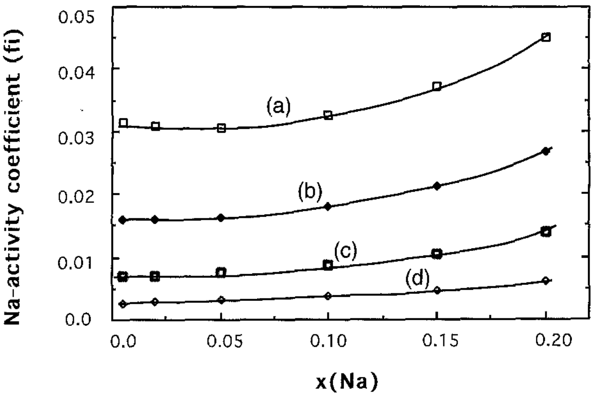

Fig. 10. Sodium activity coefficient, f_i, in Na–Pb alloys against x_{Na}. Temperatures: (a) 700, (b) 600, (c) 500 and (d) 410 °C (Itoh) [22].

4. Investigation of the AMTEC cell operated with sodium alloy electrodes

4.1. *Current–voltage curves*

Typical current–voltage characteristics of the AMTEC cell, operated with a Na–Pb alloy electrode (10 mol % Na) with no forced, but only free, thermal convection at the molten alloy cathode, are shown in Fig. 11. The temperature ranges from 500 to 700 °C. The open circuit voltages of the Na|beta″-Al_2O_3|Na–Pb (10 mol % Na) cell are almost identical for the three different temperatures. But the slopes of the current–voltage curves differ significantly, indicating increasing effective cell resistances with lower temperatures. The specific cell resistance drops from 0.45, 0.38, to 0.32 Ω cm^{-2} at 500, 600 and 700° C. This cell-resistance is the sum of the resistances of the solid electrolyte, of the contact-resistance at the phase boundaries of liquid alloy/beta″-Al_2O_3 and includes also the effect

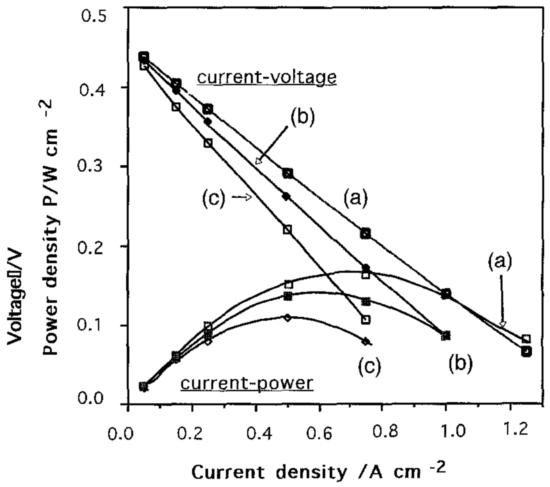

Fig. 11. Typical current–voltage (linear curves) and current–power characteristics (curves) of AMTEC with Na–Pb electrode ($A = 10\,\mathrm{cm}^{-2}$; 10 mol % Na). Temperatures: (a) 700, (b) 600 and (c) 500 °C.

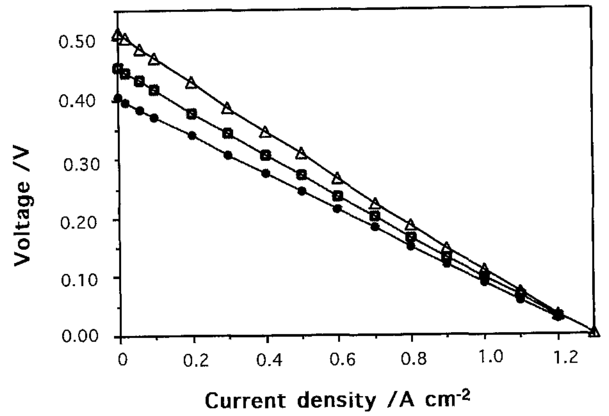

Fig. 12. Current–voltage characteristics in the Na–Pb cell with free thermal convection. $T_2 = 700\,°C$; $A = 10\,cm^2$. Concentration of Na: (△) 5, (□) 10 and (●) Na 15 mol %.

of mass transfer resistances of sodium in the alloy. All have a negative temperature dependence.

4.2. *Mass transport effect*

Figure 12 shows the current–voltage characteristics in the cell with free convection, operated with Na–Pb alloys of three different sodium concentrations at 700 °C. The current–voltage curves converge at a short-circuit current density of about $1.3\,A\,cm^{-2}$. Figure 13 shows the current–power density curves, corresponding to Fig. 12. The three different slopes correspond to apparent resistances of 0.40, 0.35 and $0.31\,\Omega\,cm^{-2}$.

Mass transport by convective diffusion in the liquid alloy electrode is a critical factor, determining the power density of a cell. Forced convection by a magnetic stirrer can reduce the effect of mass transfer on cell resistance.

Figure 14 shows the current–voltage characteristics of the AMTEC cell operated with Na–Pb alloys of three different sodium concentrations ($x_{Na} = 0.05$, 0.1 and 0.15) with a forced convection. The current–voltage curves differ considerably from those for free thermal convection. For the three sodium concentrations the resistances become almost the same (about $0.3\,\Omega\,cm^{-2}$) at sufficiently high current density. Correspondingly the current density at maximum power density shifts towards higher values and the maximum power density at $x = 0.05$ increases from 0.16 to $0.23\,W\,cm^{-2}$.

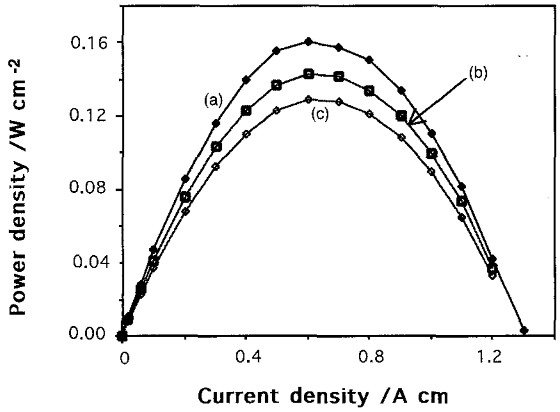

Fig. 13. Current–power characteristic in the Na–Pb cell with free thermal convection. $T_2 = 700\,°C$; $A = 10\,cm^2$. Concentration of Na: (a) 5, (b) 10 and (c) 15 mol %.

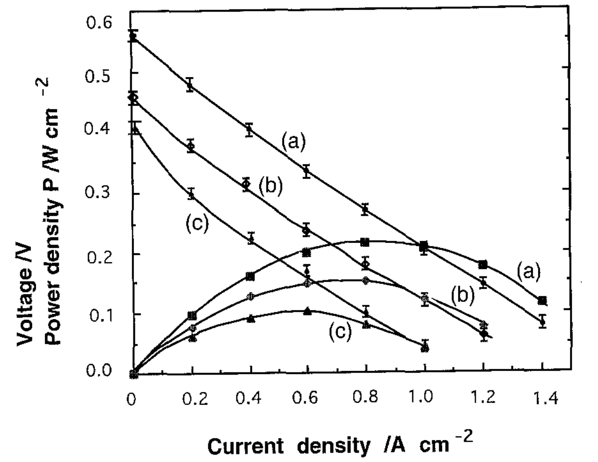

Fig. 14. Current–voltage (top curves) and current–power characteristics (lower curves) of AMTEC cell with Na–Pb cathode and forced convection. $T = 700\,°C$. Concentrations: (a) 5, (b) 19 and (c) 15 mol %.

4.3. *Maximum power densities and cell-resistances of AMTEC cells with sodium alloy cathodes and forced convection*

The impedance spectrum of an AMTEC cell with a molten Na-metal (Na–Sn or Na–Pb alloy) electrode is very simple. Since the interfacial capacitance is very small, the impedance is nothing but an ohmic resistance. This resistance is the sum of the ohmic resistances of the electrolyte and the interfacial charge transfer resistances. The resistance (impedance) depends on the temperature and the current density, but is almost independent of the Na concentration in the Na–Me alloy.

Figure 15 shows the sodium concentration dependence of the maximum power density and cell resistance of an AMTEC cell with Na–Pb alloys with forced convection at three different temperatures. The maximum power density at 0.5 mol % Na and 700 °C reaches about $0.30\,W\,cm^{-2}$. Its value decreases with increasing Na concentration. The

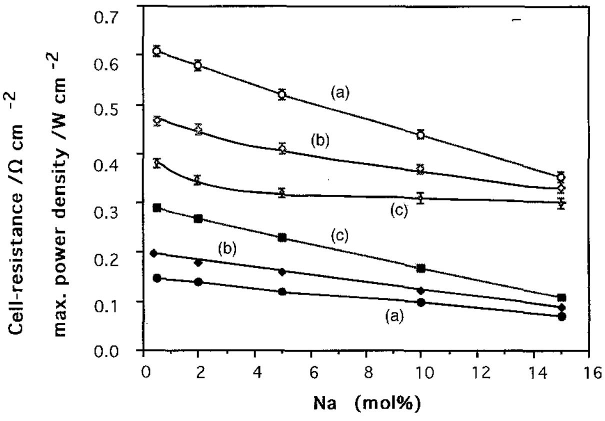

Fig. 15. Maximum power density (lower curves) and cell resistance (upper curves) for an AMTEC cell with Na–Pb cathode. $A = 10\,cm^2$. Temperatures: (a) 500, (b) 600 and (c) 700 °C.

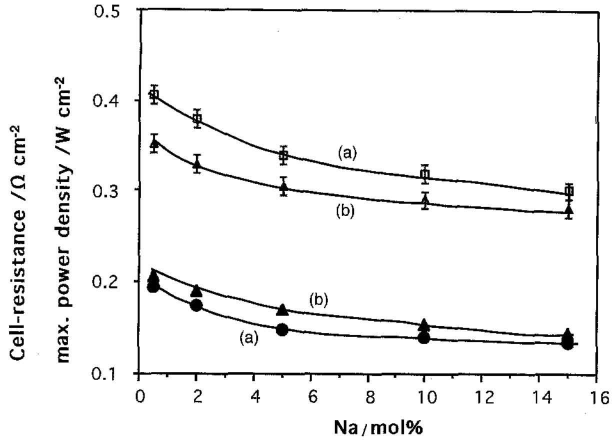

Fig. 16. Maximum power density (lower curves) and cell resistance (upper curves) for an AMTEC cell with Na–Sn cathode. $A = 10\,\text{cm}^2$. Temperatures: (a) 600 and (b) 700 °C.

effective cell resistance is almost independent of the sodium concentration at 700 °C, but becomes more sensitive with respect to concentration at lower temperatures, it decreases from 0.6 to $0.4\,\Omega\,\text{cm}^{-2}$ at 500 °C if the sodium concentration increases from $x = 0.05$ to 0.15. This indicates that for low concentration the mass transfer resistance becomes comparable to the ohmic cell resistances at low temperature.

The data in Fig. 16 which depict the results of an AMTEC cell with a Na–Sn alloy cathode, are comparable to those of the data for Na–Pb alloys. However, achieved power densities are significantly lower than for Na–Pb alloys. As the cell resistances in both cases at 700 °C are identical ($0.3\,\Omega\,\text{cm}^{-2}$), the cell impedance is likely to be solely determined by the electrolyte resistance at this temperature.

Cell resistances of 0.75, 0.66 and $0.51\,\Omega\,\text{cm}^{-2}$ for TiN, Mo and TiB_2 sputtered porous electrode by 800 °C were reported [13, 14]. Maximum power densities for an AMTEC cell with Na–Me alloy electrodes are comparable with or better than that for the sputtered Mo and TiB_2 electrodes, in which no more than $0.13\,\text{W}\,\text{cm}^{-2}$and $0.17\,\text{W}\,\text{cm}^{-2}$ at 700 °C, respectively are reported. The fact, that the AMTEC with molten alloy electrode has good power density, is due mainly to reducing the phase interfacial resistance.

5. Comparing practical and theoretical efficiency of AMTEC cells with molten Na-metal cathodes

5.1. *Calculation of the theoretical efficiency*

According to the schematic of the AMTEC-process with sodium-metal alloy cathodes (Fig. 1), five different steps which contribute different amounts of heat and one which generates electrical energy have to be accounted for. They are calculated step by step in Equations 9–14 for reversible process and the conversion of one mole of sodium.

(i) Transfer of sodium from left side of the cell to the right side,

$$W_{\text{el}} = FU_0(x) = RT_2 \ln\left(\frac{a_0}{a_{\text{i}}}\right) \tag{9}$$

$$Q_1 = T_2 \Delta S_{\text{Na(l)}} \tag{10}$$

(ii) Evaporation of sodium from the liquid alloy at T_2,

$$Q_2 = \Delta H_{\text{T}_2,\text{Na(g)}} - \Delta H_{\text{T}_2,\text{Na(l)}} \tag{11}$$

(iii) Cooling of Na vapours by the condenser to temperature T_1,

$$Q_3 = \int_{T_2}^{T_1} C_{\text{p(Na,gas)}}\,\text{d}T \tag{12}$$

(iv) Condensation of the Na vapours at T_1,

$$Q_4 = -\Delta H_{\text{T}_1,\text{Na(g)}} \tag{13}$$

(v) Heating of sodium from T_1 to T_2.

$$Q_5 = \int_{T_1}^{T_2} C_{p(\text{Na,liq.})}\,\text{d}T \tag{14}$$

From Equations 10–14, the gross conversion of heat, $\sum Q$, is obtained:

$$\begin{aligned}\sum Q = {} & T_2 \Delta S_{\text{Na(l)}}(x) + \Delta H_{\text{T}_2,\text{Na(g)}} - \Delta H_{\text{T}_2,\text{Na(l)}} \\ & + \int_{T_2}^{T_1} C_{p(\text{Na,gas})}\,\text{d}T - \Delta H_{\text{T}_1,\text{Na(g)}} \\ & + \int_{T_1}^{T_2} C_{p(\text{Na,liq.})}\,\text{d}T\end{aligned} \tag{15}$$

Considering the equation:

$$T_2 \Delta S_{\text{Na(l)}}(x) - \Delta H_{\text{T}_2,\text{Na(l)}} = \Delta G_{\text{T}_2,\text{Na(l)}}(x) = FU_0(x)$$

one obtains:

$$\begin{aligned}\sum Q = {} & FU_0(x) + \Delta H_{\text{T}_2,\text{Na(g)}} - \Delta H_{\text{T}_1,\text{Na(g)}} \\ & + \int_{T_1}^{T_2} C_{\text{p(Na-liq.)}} - C_{\text{p(Na-gas)}}\,\text{d}T\end{aligned} \tag{16}$$

It is also worth noting that the quantity of

$$\int_{T_1}^{T_2} C_{\text{p(Na-liq.)}} - C_{\text{p(Na-gas)}}\,\text{d}T \tag{17}$$

is definitely positive, because the heat released by cooling of the Na vapours is less than that for heating of the sodium-metal. Therefore, additional heat must be used for the heat transfer from Na-vapours, to heat the sodium metal from T_1 to T_2.

The total heat absorbed by the system from the high temperature heat source at T_2 is correspondingly

$$FU_0(x) + \Delta H_{T_2,\text{Na(g)}} + \int_{T_1}^{T_2} C_{\text{p(Na-liq.)}} - C_{\text{p(Na-gas)}}\,\text{d}T$$

Hence, the theoretical efficiency η_{th} of the AMTEC with sodium–metal alloy cathodes amounts to

$$\begin{aligned}\eta_{\text{th}} = {} & FU_0(x)/FU_0(x) + \Delta H_{\text{T}_2,\text{Na(g)}} \\ & + \int_{T_1}^{T_2} C_{\text{p(Na-liq.)}} - C_{\text{p(Na-gas)}}\,\text{d}T\end{aligned} \tag{18}$$

Table 4. Open circuit voltage $U_0(x)$ of AMTEC-cell with Na–Me alloy electrode (Me = Sn, Pb) and the theoretical efficiency η_{th} by 700 °C

Na/mol%	2	5	10	15	20
T_1/°C*	305	320	340	355	375
U_0(Na–Pb)/V†	0.619	0.545	0.481	0.435	0.392
η_{th}(Na–Pb)	0.389	0.360	0.332	0.310	0.289
T_1 /°C	310	330	350	370	380
U_0(Na–Sn)/V†	0.604	0.508	0.445	0.404	0.385
η_{th}(Na–Sn)	0.383	0.344	0.315	0.295	0.285

* T_1 is determined by the assumed relation: $P_{Na}(T_1) < 0.1\,P_{Na}(T_2, x)$.

† U_0 is calculated in accounting for the activity coefficients of Figs 9 and 10.

Table 4 shows the theoretical efficiencies η_{th} for the AMTEC cell operated with Na–Sn and Na–Pb alloy electrodes with various Na concentration at 700 °C. The concentration dependence of the theoretical efficiencies is depicted in Fig. 17 for the Na concentration ranges from 0.02 to 0.2. An AMTEC cell with porous film cathodes has a theoretical efficiency of approximate 40% at the two temperatures $T_2 = 700$ °C and $T_1 = 300$ °C. Its open cell voltage is about 0.8 V. For AMTEC cells with sodium alloy cathodes of low sodium content ($x = 0.02$), the theoretical efficiency matches this value, but it becomes gradually lower at the higher sodium concentration and reduces to approximate 30% at $x = 0.2$.

Of high practical importance, is the cell resistance, as open cell voltage together with the cell resistance determine achievable power densities of the cell.

6. Conclusions

Thermodynamic properties of the Na–Me (Me = Sn, Pb) molten alloys were reinvestigated by e.m.f. measurements of the Na concentration cell: Na(l)|beta″-alumina|Na–Me(l) where Me = Sn, Pb. The Na-activity, the partial molar enthalpy and partial molar entropy of dissolution for Na in molten Na–Sn and Na–Pb alloys have been investigated. The thermodynamic results for the higher temperature range 400–700 °C from this investigation are identical with that of other authors. It was found by SEM and EDS that no ion exchange reaction occurs between the beta″-alumina electrolyte and molten sodium or lead, and Na–Me molten alloys.

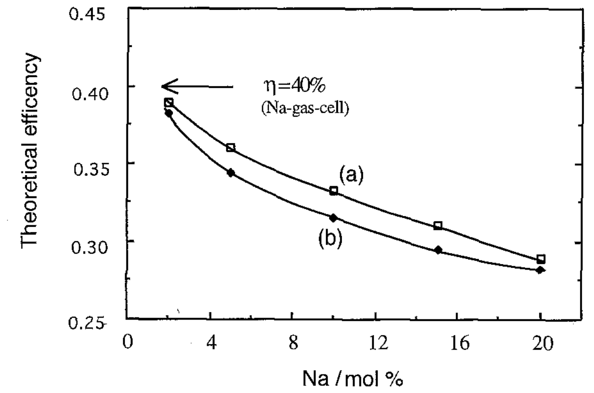

Fig. 17. Sodium concentration dependence of the theoretical efficiencies. $T_1 = 300$ °C; $T_2 = 700$ °C. Key: (a) η(Na–Pb); η(Na–Sn).

The power density of the AMTEC cell with molten alloy cathodes decreased with increasing Na concentration in the mol fraction range from 0.05 to 0.15. Maximal power densities of 0.21 to 0.15 W cm^{-2} at 700 °C for Na–Sn molten electrodes, and 0.30 to 0.15 W cm^{-2} for Na–Pb molten electrodes have been obtained. This appears favourable in comparison to values ranging from 0.13 to 0.17 W cm^{-2} at 700 °C for TiN, Mo and TiB_2 porous thin film electrodes. The electrical performance of the sodium–metal electrodes is quite satisfactory, but the obtained voltages at highest power densities appear, from a practical point of view, too low.

The volatilities of Pb and Sn are remarkably lower than that of sodium, which is useful for the separation of sodium from the alloying compounds by distillation. Na–Pb alloys are at an advantage compared to Na–Sn alloys due to the sodium activities being somewhat lower in Na–Pb than Na–Sn alloys.

The a.c. impedance data demonstrated that the molten alloy electrodes have a smaller cell resistance, 0.3–0.35 Ω cm^{-2} at 700° C. Comparison with that of the sputtered thin, porous film electrodes, indicated that the contact resistance between electrode and surface of beta″-alumina plays an important role in enhancing cell power density.

According to experimental data, the theoretical efficiency of AMTEC cell with molten sodium–metal electrode lies in the range of 30–40%, depending on Na concentration in the molten sodium–metal electrode.

Acknowledgements

Q. Fang wishes to thank Drs R. Knodler and F. Harbach for their help and understanding. Financial assistance from the Research Centre Heidelberg, ABB AG, is gratefully acknowledged.

References

[1] F. Harbach, R. Knödler and H-P. Bossmann, *Physik in unserer Zeit*, **1** (1992) 34.
[2] T. K. Hunt, N. Weber and T. Cole, Proc. 13th Intersoc. Energy Conversion Engineering Conference (1978) p. 2011.
[3] T. Cole, *Science*, **221**(4614) (1983) 915.
[4] J. T. Kummer and N. Weber, *US Patent 3 458 356* (1969).
[5] N. Weber, *Energy Convers.* **14** (1974) 1.
[6] R. M. Williams, M. E. Loveland, B. Jeffries-Nakamura, M.L. Underwood, C. P. Bankston, H. Leduc and J. T. Kummer, *J. Electrochem Soc.* **137** (1990) 1709.
[7] R. M. Williams, B. Jeffries-Nakamura, M. L. Underwood, C. P. Bankston and J. T. Kummer, *J. Electrochem Soc.* **137** (1990) 1716.
[8] H-P. Bossmann, Q. Fang, R. Knodler and F. Harbach, 'Test Cells for the Development of the AMTEC', 26th. IECEC, Boston, vol. 5, (Aug. 1991) pp. 481–86.
[9] C. P. Bankston, T. Cole, S.K. Khanna and A. P. Thakoor, 'Alkali Metal Thermoelectric Conversion (AMTEC) for Space Nuclear Power Systems' *in* 'Space Nuclear Power

Systems 1984' (edited by M. S. El-Gentz and M. D. Hoover) Orbit Book Co., Malabar, FL (1985) p. 393.

[10] T. K. Hunt, N. Weber and T. Cole, 'High Efficiency Thermoelectric Conversion with beta″-Alumina Electrolytes, the Sodium Heat Engine', *in* 'Fast Ionic Transport in Solids' (edited by J. B. Bates and G. C. Farrington) North-Holland, Amsterdam (1981) p. 263.

[11] R. M. Williams, B. Jeffries-Nakamura, M. L. Underwood, B. L. Wheeler, M. E. Loveland, S. J. Kikkert, J. L. Lamb, T. Cole, J. T. Kummer and C. P. Bankston, *J. Electrochem. Soc.* **136** (1989) 893.

[12] R. F. Novak, J. R. McBride, T. K. Hunt, D. J. Schmatz, W. B. Copple, N. Arnon and J. T. Brockway, Proc. 23rd Intersoc. Energy Conversion Engineering Conference (1988) p. 219; T. K. Hunt, Proc. 25th Intersoc. Energy Conversion Engineering Conference (1990) p. 420.

[13] Q. Fang, 'Untersuchungen zur Material- und Betriebstechnik des AMTEC' PhD thesis, Technische Hochschule, Darmstadt (1993).

[14] Q. Fang and R. Knödler, 'Porous TiB_2-electrodes for the Alkali Metal Thermoelectric Converter (AMTEC)', *J. Mater. Sci.* **27** (1992) 6725.

[15] R. Knödler, K. Reiss, B. Westhoven, *J. Mater. Sci. Lett.* **11** (1992) 343.

[16] R. Knödler, A. Kranzmann, H-P. Bossmann, F. Harbach, 'Performance of Single Cells of an Alkali Metal Thermoelectric Converter (AMTEC)', *J. Electrochem. Soc.* **139** (1992) 3030.

[17] R. C. Weast, 'Handbook of Chemistry and Physics', CRC Press, 69th edn, (1988) B99–139

[18] *Idem*, *ibid*, F-123.

[19] *Idem*, *ibid*, D193.

[20] M. Hansen and K. Anderro, 'Constitution of Binary Alloys', McGraw-Hill, New York (1958) p. 999.

[21] R. Hultgren, P. D. Desai, D. T. Hawkins, M. Gleiser and K. K. Kelley, 'Selected Values of the Thermodynamic Properties of Binary Alloys', American Society for Metals (1973).

[22] M. Itoh and Z. Kozuka, *J. Mater. Science* **26** (1991) 5221.

[23] Idem, *J. Electrochem. Soc.* **135** (1988) 2238.